JACS
JOURNAL OF THE AMERICAN CHEMICAL SOCIETY

Communication

pubs.acs.org/JACS

Nanostructured Nickel Phosphide as an Electrocatalyst for the Hydrogen Evolution Reaction

Eric J. Popczun,[†] James R. McKone,[‡] Carlos G. Read,[†] Adam J. Biacchi,[†] Alex M. Wiltrout,[†] Nathan S. Lewis,*[,‡] and Raymond E. Schaak*[,†]

[†]Department of Chemistry and Materials Research Institute, The Pennsylvania State University, University Park, Pennsylvania 16802, United States

[‡]Division of Chemistry and Chemical Engineering, California Institute of Technology, Pasadena, California 91125, United States

Supporting Information

ABSTRACT: Nanoparticles of nickel phosphide (Ni_2P) have been investigated for electrocatalytic activity and stability for the hydrogen evolution reaction (HER) in acidic solutions, under which proton exchange membrane-based electrolysis is operational. The catalytically active Ni_2P nanoparticles were hollow and faceted to expose a high density of the $Ni_2P(001)$ surface, which has previously been predicted based on theory to be an active HER catalyst. The Ni_2P nanoparticles had among the highest HER activity of any non-noble metal electrocatalyst reported to date, producing $H_2(g)$ with nearly quantitative faradaic yield, while also affording stability in aqueous acidic media.

The production of molecular hydrogen by the electrochemical reduction of water is an important component of several developing clean-energy technologies.[1,2] The hydrogen evolution reaction (HER) is effectively facilitated by noble metals such as Pt, which generate large cathodic current densities for this reaction at low overpotentials.[1,3,4] Replacement of Pt with earth-abundant metals would be desirable to facilitate the global scalability of such potential clean-energy technologies. One non-precious-metal alternative to Pt is MoS_2, which has high HER activity and exhibits good stability in acidic solutions.[3] MoB and Mo_2C have also been identified as active HER catalysts in both acidic and alkaline solutions.[5,6] The first-row metal nickel, which is significantly more abundant than Mo, is often used as an electrocatalyst for the HER, with active electrocatalysts produced by use of alloys such as Ni–Mo,[7−9] Ni–Mo–Zn,[10] Ni–Fe,[9] and Ni–P.[11,12] These Ni-based catalysts are not, however, stable in acidic solutions, in which proton exchange membrane-based electrolysis is feasible and operational. Addition of nitrogen to Ni–Mo, to form Ni–Mo–N composites, has been shown to significantly improve the acid stability of such alloys,[13] but such systems still show significantly lower HER activity and/or stability in acidic solutions than noble metals such as Pt.

MoS_2, an active earth-abundant HER electrocatalyst, is also highly active for hydrodesulfurization (HDS).[3,14] Both HDS and the HER rely on the catalyst to reversibly bind H_2, with H_2 dissociating to produce H_2S in HDS and with protons bound to the catalyst to promote the formation of H_2 in the HER.[15−17] The putative active sites of MoS_2 for HDS are the under-coordinated edges as opposed to the basal planes.[14,18] Similarly, for the HER, the most active sites of MoS_2 are believed to be the $(10\bar{1}0)$ planes that are exposed on the edges, rather than the (0001) basal planes.[19,20] These commonalities between the mechanisms and putative active sites of MoS_2 for both HDS and HER catalysis suggest that other materials that are known HDS catalysts may also provide active electrocatalysts for the HER.

Nickel phosphide (Ni_2P), which adopts the hexagonal Fe_2P structure (Figure 1A),[21] is a well-known HDS catalyst,[16,22] and

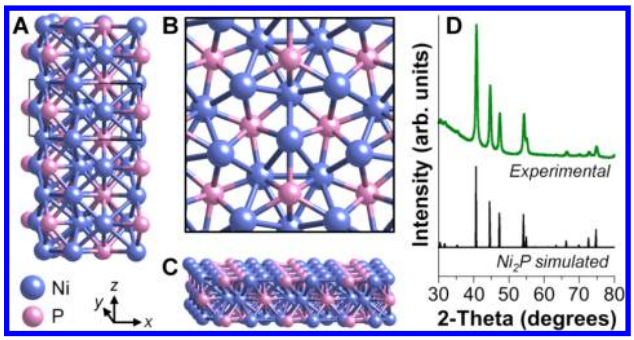

Figure 1. Crystal structure of Ni_2P: (A) four unit cells stacked on top of one another, with a single unit cell outlined, (B) top-down view of the $Ni_2P(001)$ surface, and (C) a two-dimensional slice of Ni_2P, showing the (001) surface on top. (D) Experimental powder XRD pattern for the Ni_2P nanoparticles (top), with the simulated pattern of Ni_2P shown for comparison (bottom).

Ni_2P also produces $H_2(g)$ via the water–gas shift reaction.[23] Additionally, density functional theory calculations have indicated that the $Ni_2P(001)$ surface, which has exposed Ni and P sites (Figure 1B,C), exhibits an ensemble effect, whereby proton-acceptor and hydride-acceptor centers are both present to facilitate catalysis of the HER.[17] $Ni_2P(001)$ has also been shown to have structural and electronic analogies to the active site of [NiFe] hydrogenase, which is a highly active biological HER catalyst.[17] $Ni_2P(001)$ has furthermore been identified as a potential HER catalyst that could merge the activity of [NiFe] hydrogenase with the thermostability of a heterogeneous catalyst.[17] Motivated by these predictions, herein we report

Received: April 6, 2013

   dx.doi.org/10.1021/ja403440e | J. Am. Chem. Soc. XXXX, XXX, XXX–XXX

that nanostructured Ni_2P is an active HER electrocatalyst that is comprised entirely of inexpensive and earth-abundant elements while exhibiting improved performance and stability relative to other comparable earth-abundant electrocatalysts.

Ni_2P nanoparticles were synthesized by heating nickel(II) acetylacetonate [$Ni(acac)_2$] in 1-octadecene, oleylamine, and tri-*n*-octylphosphine (TOP) to 320 °C for 2 h, cooling to room temperature, washing with ethanol and hexanes, and isolating by centrifugation.[24,25] [***Caution!*** *High-temperature decomposition of a phosphine can liberate phosphorus, so this reaction should be considered as highly corrosive and flammable and therefore should only be carried out by appropriately trained personnel, under rigorously air-free conditions.*] Figure 1D shows the powder X-ray diffraction (XRD) pattern of the nanoparticles, confirming the formation in high yield of Fe_2P-type Ni_2P. Scherrer analysis of the peak widths indicated an average grain size of 17 nm. Consistent with the Scherrer analysis, transmission electron microscope (TEM) images (Figure 2A) revealed quasi-spherical nanoparticles with an average diameter of 21 ± 2 nm. The corresponding energy dispersive X-ray (EDX) spectrum (Figure 2B) verified that Ni and P were present in a 2:1 ratio, and the corresponding selected area electron diffraction pattern (Figure S1) confirmed that the nanoparticles were Fe_2P-type Ni_2P.

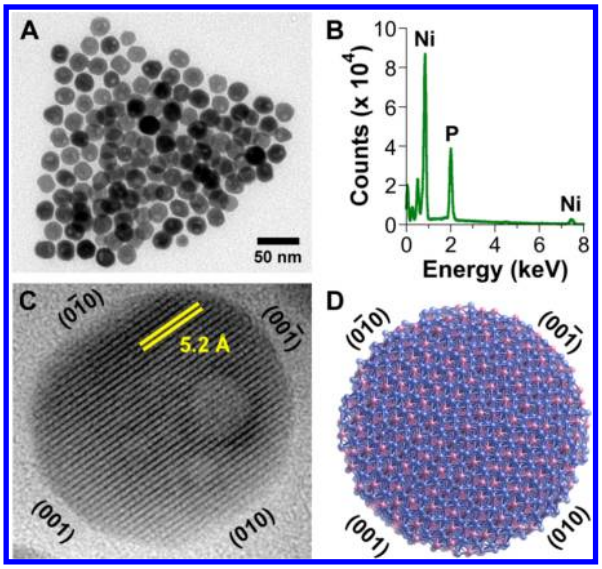

Figure 2. (A) TEM image and (B) EDX spectrum of Ni_2P nanoparticles. (C) HRTEM image of a representative Ni_2P nanoparticle, highlighting the exposed $Ni_2P(001)$ facet and the 5.2-Å lattice fringes that correspond to the (010) planes. (D) Proposed structural model of the Ni_2P nanoparticles.

The Ni_2P nanoparticles were hollow and multifaceted, as revealed by close inspection of the TEM images (Figure 2A). Hollow nanoparticles of colloidal Ni_2P form in solution from the reaction of Ni nanoparticles with phosphorus, which is liberated from the decomposition of TOP, via a nanoscale Kirkendall pathway.[24−27] High-resolution (HR) TEM images (Figure 2C) showed that the Ni_2P nanoparticles were single crystalline and faceted. The observed 5.2-Å lattice fringes correspond to the (100) and (010) planes of Ni_2P, indicating that the nanoparticle surfaces exposed, among other facets, the $Ni_2P(001)$ crystal planes (Figure 2D) that have been predicted to have the highest activity for the HER.[17]

Figure 3 shows the electrocatalytic activity of the Ni_2P nanoparticles in a standard electrochemical configuration in

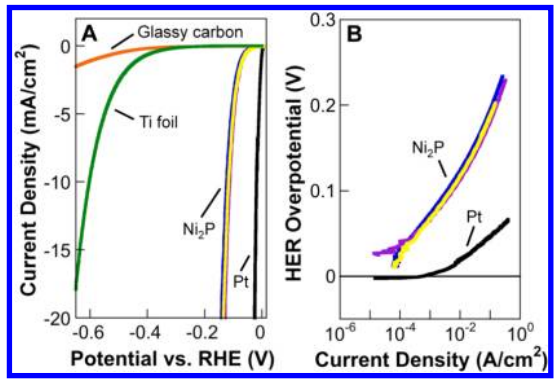

Figure 3. (A) Polarization data for three individual Ni_2P electrodes in 0.5 M H_2SO_4, along with glassy carbon, Ti foil, and Pt in 0.5 M H_2SO_4, for comparison. (B) Corresponding Tafel plots for the Ni_2P and Pt electrodes.

0.50 M H_2SO_4, with the working electrode (Figure S2) prepared by deposition of the Ni_2P nanoparticles at a mass loading of ~1 mg/cm^2 onto a 0.20 cm^2 Ti foil substrate. To remove the organic ligands that capped the surface of the nanoparticles, the as-prepared Ni_2P/Ti electrode was heated for 30 min at 450 °C in 5% H_2/N_2 (Figure S2). Diffuse reflectance infrared Fourier transform spectroscopy (DRIFTS) of the as-prepared electrode revealed peaks at 2924 and 2854 cm^{-1} that correspond to C−H stretching modes (Figure S2). After annealing, these peaks disappeared, and no peaks attributable to the functional groups of any of the organic components, or their organic decomposition products, were observed. For comparison, Figure 3 also displays the HER activity of nanoparticles of Pt, which is known to be a highly active electrocatalyst for the HER.[1,3,4] As expected, neither bare Ti foil nor glassy carbon showed significant HER activity (Figure 3) over this range of electrode potentials.

More than 20 individual Ni_2P electrodes were tested, and their HER activities were highly consistent, as illustrated by the results displayed in Figure 3 for three consecutive electrodes. In 0.50 M H_2SO_4, the overpotentials (η) required for the Ni_2P nanoparticle films to produce cathodic current densities (j) of 20 and 100 mA/cm^2 were η = 130 mV and η = 180 mV, respectively. These overpotentials compare favorably to the behavior of other non-Pt HER electrocatalysts in acidic aqueous solutions with similar mass loadings, including bulk Mo_2C and MoB,[5] Mo_2C nanoparticles deposited on carbon nanotube supports,[6] MoS_2 nanoparticles anchored on reduced graphene oxide,[28] and unsupported Ni−Mo−N nanosheets.[13] These catalyst systems exhibit overpotentials that range from 140 to 240 mV at cathodic current densities of 10−20 mA/cm^2. (See Supporting Information for specific comparisons.) Ni−Mo nanopowder has a higher initial activity (η = 80 mV for j = −20 mA/cm^2) than Ni_2P, but the activity of Ni−Mo degrades rapidly under acidic conditions.[29]

Figures 3b and S3 display Tafel plots [overpotential vs log(current density)] for Ni_2P and Pt. The Pt electrode exhibited a Tafel slope of ~30 mV/decade and an exchange current density of 2.7 × 10^{-3} A/cm^2. Both parameters are consistent with the high activity and the known mechanism of the HER on Pt. The bare titanium substrate, which had also been subjected to the same H_2/N_2 heat treatment as the Ni_2P/

dx.doi.org/10.1021/ja403440e | J. Am. Chem. Soc. XXXX, XXX, XXX−XXX

Ti electrode, was not significantly active for the HER, displaying an exchange current density of 3.3×10^{-6} A/cm^2 and a Tafel slope of 170 mV/decade. Tafel analysis of the Ni_2P nanoparticles in 0.50 M H_2SO_4 indicated an exchange current density of 3.3×10^{-5} A/cm^2 and a Tafel slope of ~46 mV/decade in the region of η = 25−125 mV. At higher overpotentials (η = 150−200 mV), the Tafel slope and exchange current density increased to ~81 mV/decade and 4.9×10^{-4} A/cm^2, respectively. These values do not match the expected Tafel slopes of 29, 38, and 116 mV/decade, each of which correlate with a different rate-determining step of the HER.[15] However, the 46 mV/decade Tafel slope at low overpotentials is comparable to the values observed for other nanostructured HER catalysts, including MoS_2 nanoparticles supported on reduced graphene oxide (41 mV/decade),[28] porous MoS_2 that exposes a high density of HER active sites (50 mV/decade),[30] and Mo_2C/carbon nanotube composites (55 mV/decade).[6] The 81 mV/decade Tafel slope at higher overpotentials is close to that of unsupported MoS_2 nanoparticles (94 mV/decade).[28]

The turnover frequencies (TOFs) for the HER in 0.50 M H_2SO_4 were estimated for η = 100 mV and η = 200 mV using both theoretical and experimental surface areas, in which each individual atom on the outermost surface layer was treated as a potential active site for the reaction.[29] These calculations thus represent only an estimate of the actual TOFs because the calculation does not account for surface area obscured by interparticle contacts or for porosity. Additionally, the specific active sites of Ni_2P are not known explicitly. Using the experimentally determined Brunauer−Emmett−Teller (BET) surface area of 32.8 ± 0.2 m^2/g for the hollow Ni_2P nanoparticles, the TOFs (per surface atom) were calculated to be 0.015 s^{-1} at η = 100 mV and 0.50 s^{-1} at η = 200 mV. Theoretical TOF values, estimated geometrically by assuming 20-nm spherical particles of Ni_2P, were 0.012 s^{-1} at η = 100 mV and 0.40 s^{-1} at η = 200 mV. These calculated TOF values are in close agreement with one another and are similar to those estimated for Ni−Mo nanopowders operated under alkaline conditions, for which TOF = 0.05 s^{-1} at η = 100 mV and TOF = 0.36 s^{-1} at η = 200 mV.[29]

The faradaic yields for H_2 evolution of the Ni_2P nanoparticles and of the Pt nanoparticles were estimated by maintaining catalyst-loaded Ti foil working electrodes (0.20 cm^2 surface area, 1 mg/cm^2 loading) at a cathodic current of 10 mA for 50 min, resulting in passage of 30 C of charge. Over 50 min (3000 s), Ni_2P and Pt produced identical amounts of H_2, and the amount of H_2 evolved agreed closely with the theoretical value based on Faraday's law, implying a quantitative faradaic yield. While some corrosion of Ni_2P was observed (Figure S5), complete corrosion, for example to phosphine or phosphates and Ni(II), would result in a quantity of gas equivalent to <5% of the observed gas yield. Hence the Ni_2P was capable of sustained electrocatalytic hydrogen production in acidic solutions, consistent with the known resistance of metal-rich phosphides to dissolution in aqueous acids.[31]

Accelerated degradation studies were performed to further evaluate the stability of the Ni_2P nanoparticles during electrocatalytic hydrogen evolution in 0.50 M H_2SO_4.[13] Cyclic voltammetric (CV) sweeps between +0.22 and −0.23 V (vs the reversible hydrogen electrode potential, RHE) were applied to the Ni_2P-decorated working electrodes (Figure S4). After 500 CV sweeps, the overpotential required to achieve current densities of 20 mA/cm^2 and 100 mA/cm^2 increased by less than 25 and 50 mV, respectively (Figure 4). Hence the overpotential increased from 130 to 155 mV at a current density of 20 mA/cm^2. After similar testing, most other Ni-based HER catalysts, including Ni and Ni−Mo, exhibit little to no HER activity due to their chemical instability toward aqueous acids.[13,29] After the degradation study, the activity of the nanostructured Ni_2P catalyst was comparable to that of MoS_2 nanoparticles deposited on reduced graphene oxide (η = 150 mV for j = 10 mA/cm^2, loading = 0.28 mg/cm^2, 0.50 M H_2SO_4).[28] The Ni_2P nanoparticles also catalyzed the HER in alkaline solutions, exhibiting an overpotential of 205 mV at a cathodic current density of 20 mA/cm^2 (Figure S6). However, the Ni_2P quickly degraded to Ni in 1.0 M KOH, and the HER performance declined rapidly.

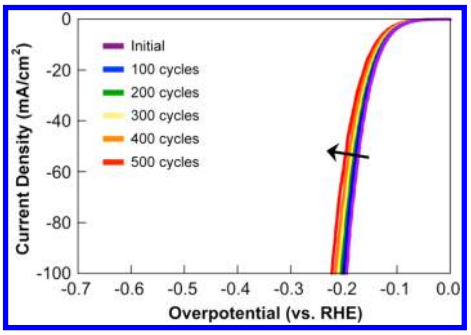

Figure 4. Polarization data for Ni_2P samples in 0.5 M H_2SO_4 initially and after 100, 200, 300, 400, and 500 CV sweeps between +0.22 and −0.23 V vs RHE.

In summary, nanostructured Ni_2P, with a high accessible surface area and a high density of exposed (001) facets that have been predicted to be active for catalyzing the HER,[17] is indeed an active HER electrocatalyst. Because Ni_2P is also a well-known HDS catalyst (as is MoS_2), these observations suggest that other known HDS catalysts are also interesting candidates for identifying new highly active, earth-abundant HER electrocatalysts. Furthermore, chemical substitution and additional nanostructuring efforts, both of which have been demonstrated to improve catalytic HDS performance,[22] are promising routes to possibly obtaining further improvement in the HER activity of Ni_2P, as well understanding in detail the relationship between the HER activity and the quantity and characteristics of different exposed facets of Ni_2P in such systems.

■ ASSOCIATED CONTENT

Supporting Information

Complete experimental details, additional characterization data, and comparison with other HER catalysts. This material is available free of charge via the Internet at http://pubs.acs.org.

■ AUTHOR INFORMATION

Corresponding Author

schaak@chem.psu.edu; nslewis@caltech.edu

Notes

The authors declare no competing financial interest.

■ ACKNOWLEDGMENTS

This work was supported by the U.S. National Science Foundation "Powering the Planet" Center for Chemical Innovation (CHE-0802907). J.R.M. acknowledges the Depart-

ment of Energy, Office of Science for a graduate research fellowship. TEM imaging was performed in the Electron Microscopy Facility of the Huck Institutes of the Life Sciences, and HRTEM and SEM imaging was performed in the Materials Characterization Lab of the Penn State Materials Research Institute. The authors thank Melisa Yashinski, Julie Anderson, and Trevor Clark for assistance with SEM imaging, Josh Stapleton for assistance with DRIFTS data collection and interpretation, and Jason Binz and Robert Rioux for assistance with the BET surface area measurements.

REFERENCES

(1) Walter, M. G.; Warren, E. L.; McKone, J. R.; Boettcher, S. W.; Mi, Q.; Santori, E. A.; Lewis, N. S. *Chem. Rev.* **2010**, *110*, 6446.
(2) Lewis, N. S.; Nocera, D. G. *Proc. Natl. Acad. Sci. U.S.A.* **2006**, *103*, 15729.
(3) Merki, D.; Hu, X. *Energy Environ. Sci.* **2011**, *4*, 3878.
(4) Gray, H. B. *Nature Chem.* **2009**, *1*, 7.
(5) Vrubel, H.; Hu, X. *Angew. Chem.* **2012**, *124*, 12875.
(6) Chen, W.-F.; Wang, C.-H.; Sasaki, K.; Marinkovic, N.; Xu, W.; Muckerman, J. T.; Zhu, Y.; Adzic, R. R. *Energy Environ. Sci.* **2013**, *6*, 943.
(7) Brown, D. E.; Mahmood, M. N.; Turner, A. K.; Hall, S. M.; Fogarty, P. O. *Int. J. Hydrogen Energy* **1982**, *7*, 405.
(8) Brown, D. E.; Mahmood, M. N.; Man, M. C.; Turner, A. K. *Electrochim. Acta* **1984**, *29*, 1551.
(9) Raj, I. A.; Vasu, K. I. *J. Appl. Electrochem.* **1990**, *20*, 32.
(10) Nocera, D. G. *Acc. Chem. Res.* **2012**, *45*, 767.
(11) Paseka, I. *Electrochim. Acta* **1995**, *40*, 1633.
(12) Burchardt, T. *Int. J. Hydrogen Energy* **2001**, *26*, 1193.
(13) Chen, W.-F.; Sasaki, K.; Ma, C.; Frenkel, A. I.; Marinkovic, N.; Muckerman, J. T.; Zhu, Y.; Adzic, R. R. *Angew. Chem., Int. Ed.* **2012**, *51*, 6131.
(14) Prins, R.; De Beer, V. H. J.; Somorjai, G. A. *Catal. Rev.* **1989**, *31*, 1.
(15) Bockris, J. O. M.; Potter, E. C. *J. Electrochem. Soc.* **1952**, *99*, 169.
(16) Liu, P.; Rodriguez, J. A.; Asakura, T.; Gomes, J.; Nakamura, K. *J. Phys. Chem. B* **2005**, *109*, 4575.
(17) Liu, P.; Rodriguez, J. A. *J. Am. Chem. Soc.* **2005**, *127*, 14871.
(18) Chianelli, R. R.; Siadati, M. H.; Perez De La Rosa, M.; Berhault, G.; Wilcoxon, J. P.; Bearden, R., Jr.; Abrams, B. L. *Catal. Rev.* **2007**, *48*, 1.
(19) Jaramillo, T. F.; Jorgensen, K. P.; Bonde, J.; Nielsen, J. H.; Horch, S.; Chorkendorff, I. *Science* **2007**, *317*, 100.
(20) Karunadasa, H. L.; Montalvo, E.; Sun, Y.; Majda, M.; Long, J. R.; Chang, C. J. *Science* **2012**, *335*, 698.
(21) Rundqvist, S. *Acta Chem. Scand.* **1962**, *4*, 992.
(22) Prins, R.; Bussell, M. E. *Catal. Lett.* **2012**, *142*, 1413.
(23) Liu, P.; Rodriguez, J. A.; Takashiri, Y.; Nakamura, K. *J. Catal.* **2009**, *262*, 294.
(24) Wang, J.; Johnston-Peck, A. C.; Tracy, J. B. *Chem. Mater.* **2009**, *21*, 4462.
(25) Muthuswamy, E.; Savitha, G. H. L.; Brock, S. L. *ACS Nano* **2011**, *5*, 2402.
(26) Henkes, A. E.; Vasquez, Y.; Schaak, R. E. *J. Am. Chem. Soc.* **2007**, *129*, 1896.
(27) Chiang, R.-K.; Chiang, R.-T. *Inorg. Chem.* **2007**, *46*, 369.
(28) Li, Y.; Wang, H.; Xie, L.; Liang, Y.; Hong, G.; Dai, H. *J. Am. Chem. Soc.* **2011**, *133*, 7296.
(29) McKone, J. R.; Sadtler, B. F.; Werlang, C. A.; Lewis, N. S.; Gray, H. B. *ACS Catal.* **2013**, *3*, 166.
(30) Kibsgaard, J.; Chen, Z.; Reinecke, B. N.; Jaramillo, T. F. *Nat. Mater.* **2012**, *11*, 963.
(31) Aronsson, B.; Lundstrom, T.; Rundqvist, S. *Borides, Silicides, and Phosphides: A critical review of their preparation, properties and crystal chemistry*, 1st ed.; Wiley & Sons: New York, 1965.